Journal of Structural Geology, Vol. 5, No. 5, pp. 519 to 538, 1983
Printed in Great Britain

0191-8141/83 $03.00+0.00
Pergamon Press Ltd.

The structure and tectonic evolution of the Aguilón fold-nappe, Sierra Alhamilla, Betic Cordilleras, SE Spain

J. P. PLATT

Department of Geology and Mineralogy, Oxford University, Parks Road, Oxford OX1 3PR, U.K.

B. VAN DEN EECKHOUT,* E. JANZEN,† G. KONERT,‡ O. J. SIMON and R. WEIJERMARS

Geological Institute, University of Amsterdam, Nieuwe Prinsengracht 130, Amsterdam, The Netherlands

(*Received* 3 *December* 1982; *accepted in revised form* 20 *May* 1983)

Abstract—Detailed structural work in the Sierra Alhamilla, SE Spain, shows that the Aguilón nappe, comprising Triassic and older metasedimentary rocks, is a fold-nappe. The most prominent set of small-scale folds changes from dominantly N-vergent in the upper, right-way-up limb to S-vergent in the greatly thinned lower limb. The nappe closes to the north, and must have been emplaced in this direction. Nappe formation was accompanied by small-scale folding and extensive solution-transfer producing a pronounced differentiated crenulation cleavage. These structures overprint an earlier set of folds and cleavage, and are overprinted in turn by late N-vergent structures. The lower limb of the nappe was thinned and disrupted during continued nappe transport.

Pre-Triassic schist in the core of the nappe was affected by medium-grade metamorphism of probable post-Triassic age. The contact with low-grade Permo-Triassic sediments above and below the schist coincides with a distinct change in metamorphic grade. This contact may be a post-metamorphic extensional fault that is now folded around the nappe, which suggests that nappe formation was preceded by extensional faulting. This is consistent with gravity spreading as the driving process for nappe emplacement.

INTRODUCTION

THE BETIC orogen (Fig. 1) in southern Spain is part of the peri-Mediterranean orogenic system, and is a consequence of the complicated pattern of motions between the African and European plates since early Jurassic time (Dewey *et al.* 1973). The orogen comprises three main units.

(1) *A Neogene fold-belt in the northeast (Prebetic Zone).* This unit was formed by thin-skinned compressional tectonics in a Mesozoic to Tertiary platform and shelf sequence (García-Hernández *et al.* 1980).

(2) *A complicated central belt of non-metamorphic Mesozoic and Tertiary sediments (Subbetic Zone).* This unit includes the southern edge of the Iberian shelf, and was the locus of Triassic to mid-Jurassic rifting, and Cretaceous to early Tertiary deep-water sedimentation (Hermes 1978). Subbetic sediments were thrust northwards onto the Prebetic in Neogene time (García-Hernández *et al.* 1980).

(3) *The mainly metamorphic Betic Zone in the south.* This unit consists mainly of Triassic and older clastic metasediments overlain by mid to late Triassic carbonate rocks of platform facies, which were involved in large-scale nappe tectonics before the middle Miocene (Egeler & Simon 1969).

During Neogene and Quaternary time the Betic Cordilleras were considerably disrupted by wrench faulting and block and basin formation.

The nappes of the Betic Zone are traditionally grouped into several 'complexes', although definitive criteria for distinguishing them are difficult to establish (Egeler & Simon 1969, Egeler *et al.* 1971, Torres-Roldán 1979). The lowest complex is the Nevado-Filabride Complex (Figs. 1 and 2) the upper units of which were affected by glaucophane–schist to eclogite facies metamorphism, subsequently overprinted by upper greenschist to amphibolite metamorphism of intermediate P/T ratio type (Nijhuis 1964, de Roever & Nijhuis 1963, Diaz de Federico *et al.* 1978). As pointed out by Torres-Roldán (1979), this metamorphic evolution helps to distinguish the Nevado-Filabrides from the overlying complexes (grouped as Higher Betic Nappes in Fig. 1). The latter include the Alpujarrides (variable metamorphic grade, evolution from medium to low P/T ratio metamorphism) and the overlying Malaguides (low grade to unmetamorphosed).

Outstanding problems in the Betic Zone concern the relative timing of nappe emplacement, the metamorphic history and the intensive polyphase ductile deformation. The nappes have traditionally been regarded as simple thrust-sheets (Egeler & Simon 1969, Torres-Roldán 1979), the formation of which was unrelated to their internal deformation. Hence no structural evidence could be adduced about their sense of emplacement. Discussions of nappe provenance depended mainly on palaeogeographic arguments based on Palaeozoic (Borrouilh & Gorsline 1979) and Triassic (Egeler & Simon

Present addresses:
* Institute for Earth Sciences, University of Utrecht, Budapestlaan 4, 3508 TA Utrecht, The Netherlands.
† c/o U.N.D.P. Boîte Postale 1490, Bujumbura, Burundi, Africa.
‡ c/o Shell International Petroleum Company, Postbox 162, The Hague, The Netherlands.

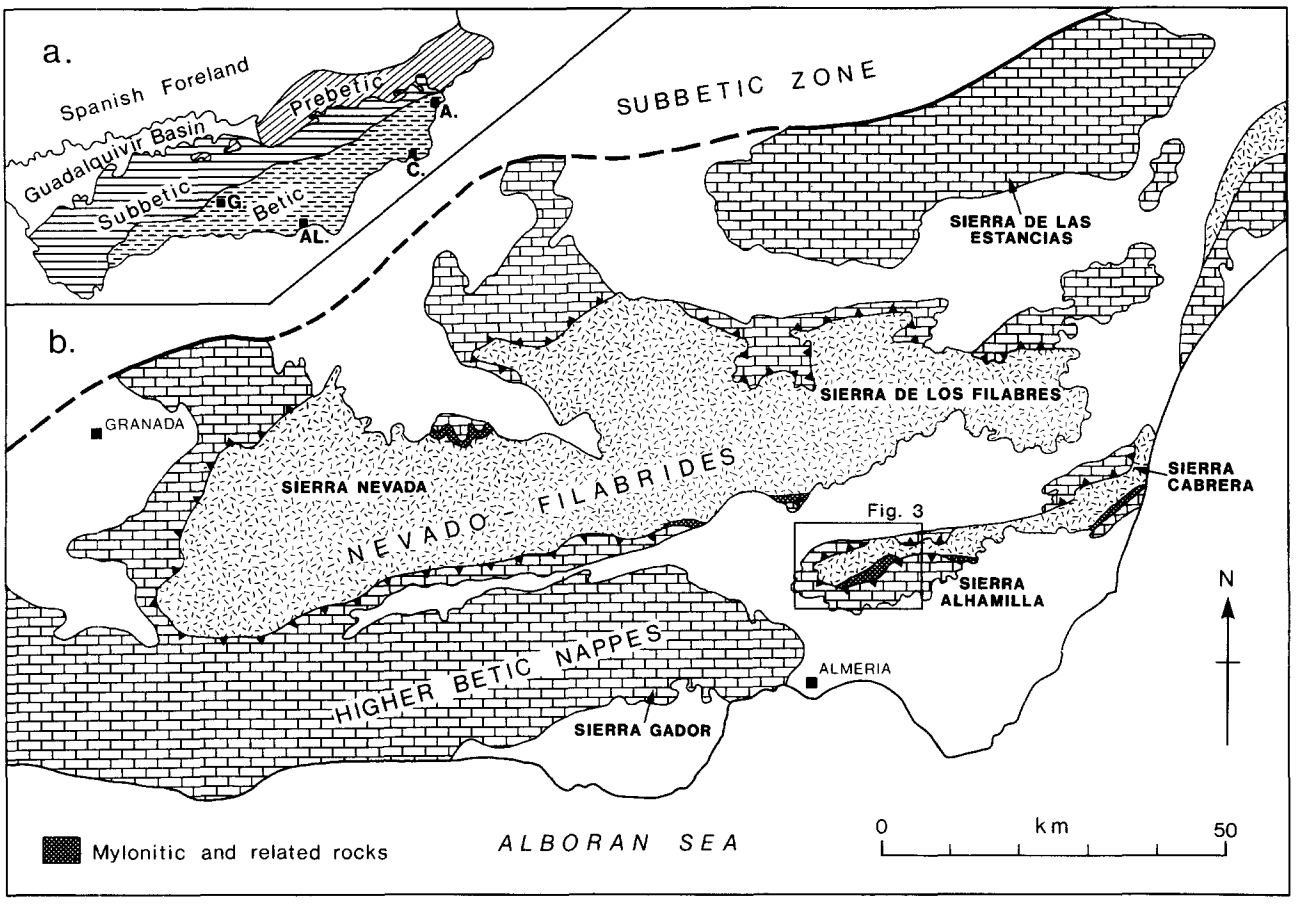

Fig. 1. (a) Tectonic subdivisions of the Betic Cordilleras, Southern Spain. A, Alicante; C, Cartagena; Al, Almería; G, Granada. (b) Tectonic sketch map of the eastern Betic Zone. 'Higher Betic Nappes' include Alpujarride and Malaguide Complexes. Known outcrops of mylonitic rocks shown by dense stipple.

1969) facies distributions, which are controversial and unlikely to have been related to the later Mesozoic basins or the Tertiary orogenic trends. The precise sense of nappe emplacement is particularly critical in view of the uncertain origin of the Betic–Rif orocline, and the lack of any clearcut plate tectonic model for the western Mediterranean (Andrieux *et al.* 1972, Kampschuur & Rondeel 1975, Torres-Roldán 1979).

The purpose of this paper is to document the existence of a fold-nappe in the Betic Zone. The large-scale geometry, as deduced from small-scale structures, indicates a northerly sense of emplacement. An important phase of ductile deformation accompanied nappe formation, and this allows the metamorphic and microstructural history to be related to the large-scale tectonics.

GEOLOGICAL SETTING

The Sierra Alhamilla is an isolated range in the southeastern Betic Cordilleras, northeast of Almería (Fig. 1). The topography is controlled by the major structure: an E–W trending anticlinorium, plunging at its western termination, and bounded to the north by high-angle faults (Figs. 3–5). This structure was formed after the Miocene: clastic sediments of Tortonian age are folded around the anticlinorium, faulted and locally overturned on the north side, and preserved in a graben within the range (Fig. 15). These sediments unconformably overlie the metamorphic rocks forming the bulk of the range. The latter comprise two main tectonic units; (a) the Alhamilla Unit which is overlain by (b) the Aguilón

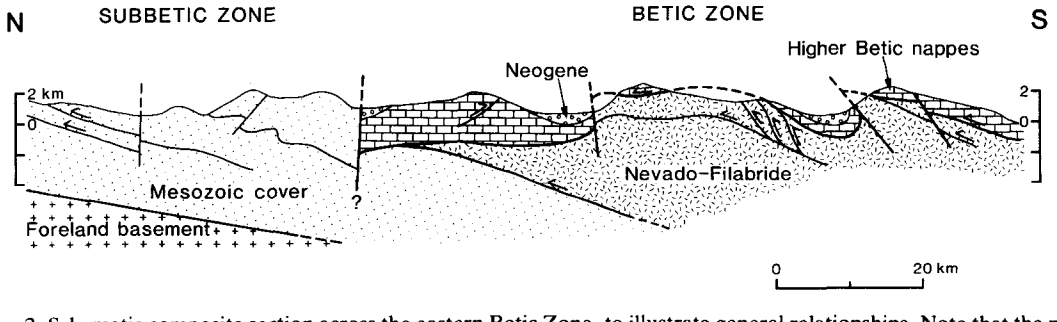

Fig. 2. Schematic composite section across the eastern Betic Zone, to illustrate general relationships. Note that the nappe structures have been considerably disturbed by later folds and normal, reverse and strike-slip faults, which formed during Neogene sedimentation.

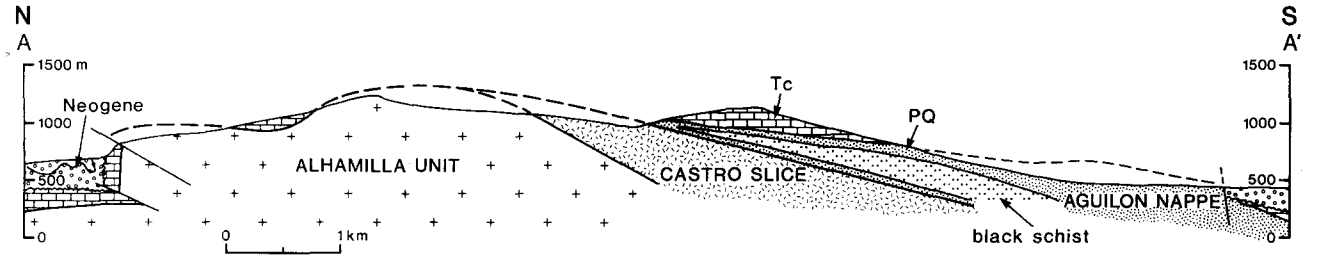

Fig. 4. Simplified cross-section A–A′ across the Sierra Alhamilla (see Fig. 3 for location). Ornament as in Fig. 3. Tc, Triassic dolomite; PQ, multicoloured phyllite and quartzite. See also Figs. 5 and 7 for more detail from the northern and southern parts of the section.

nappe. The Alhamilla Unit consists of low grade graphitic mica–schist and quartzite, and the medium grade Castro slice, which includes marble and quartz–felspar gneiss. The rocks are unfossiliferous and of unknown age. They have been affected by mylonitic and cataclastic deformation related to nappe emplacement (Behrmann & Platt 1982, Platt 1982), and their structure will be described in detail by Platt & Behrmann (in prep.). The lithological assemblage closely resembles rocks in the Sierra de los Filabres and the Sierra Nevada, and the unit may be part of the Nevado-Filabride Complex.

We distinguish the overlying Aguilón nappe primarily on structural grounds: it forms a recumbent fold with an inverted limb that lies discordantly on the Alhamilla Unit. It consists largely of a distinctive assemblage of low-grade Permo-Triassic metasediments characteristic of the Alpujarride Complex, but it includes a body of medium-grade graphitic mica–schist in its core.

In the western Sierra Alhamilla, there are thrust slices of Permo-Triassic rocks sufficiently different in character from those in the Aguilón nappe to suggest to some of us (B.v.d.E. and O.J.S.) that they may be remnants of higher nappes. The principal outcrops are annotated in Fig. 3 with the letters S (Savín Unit) and P (Las Palmas Unit). These units comprise reddish shale and sandstone, dark-grey dolostone, and gypsum, and they show a lower degree of metamorphic recrystallization than the rocks of the Aguilón nappe.

ROCK-TYPES AND STRATIGRAPHY OF THE AGUILÓN NAPPE

The nappe consists of a semi-concordant sequence of rock types, which is best developed in the south of the Sierra (Figs. 3 and 4). From top to bottom there are five units within the structural sequence.

(a) Up to 200 m stratigraphic thickness of carbonate rocks: largely grey and black dolostone, with interlayers of grey limestone. The dolostone is commonly extensively brecciated and veined, which obscures the bedding and internal structure. At the base, which is commonly a décollement surface, there may be up to 30 m of platy yellow and grey limestone and calcareous yellow phyllite, overlying a further 15 m of grey limestone and dolostone. This basal packet contains abundant bivalves (*Lyriomyophoria betica* [Hirsch]), and has been dated as Middle Triassic (Ladinian) using ostracods (Kozur *et al.* 1974).

(b) About 150 m, but locally up to 400 m, structural thickness of strongly folded low-grade pink or red phyllite and quartzite (PQ). Quartzite shows clastic sedimentary textures (Fig. 10a), and well-developed tabular cross-bedding. Near the base, deformation has largely obscured the sedimentary textures, and the colour fades to light grey or green. A 10-m interlayer of dolostone breccia crops out near Rambla del Agua (626897 and 646900 on the Almería 1:50,000 topographic sheet 23-43).

(c) A discontinuous unit of black graphitic quartz–mica–schist, with a present structural thickness of up to 250 m, consisting of 2 cm to 2 m thick grey psammite layers interlayered with black pelitic schist. A few thin marble layers occur, for example Rambla del Agua (626914). The rocks have a coarse crystalline texture with porphyroblasts of garnet and staurolite up to 1 cm in diameter.

(d) Up to 100 m of phyllite, quartzite and fine grained quartz–muscovite schist. The rocks are strongly foliated and sedimentary textures have been obscured by deformation. The quartzite is white or light green; the phyllite is generally steel-grey, but may be coloured green, purple or black by small amounts of chlorite and iron oxides. Around Baños (540910) it is bleached and kaolinized. Locally (e.g. Barranco de Castro, 623916), small pods of chlorite schist occur. The unit is similar to the lower part of unit (b), and where the black schist is missing, as in the west and north, the upper and lower phyllite–quartzite units cannot be distinguished.

(e) 0.5–10 m of carbonate rocks, locally absent, and variable in character. They are best developed in the west, around Baños (540910), where they form massive dolomite–ankerite rocks, locally including large amounts of siderite, goethite and haematite. Further east the zone is thinner, and appears as a layer of calcite–dolomite mylonite, or as cargneule (porous calcite–dolomite breccia), with porphyroclasts of dolostone, and tectonic blocks up to several metres in diameter of mylonitic schist.

This sequence of five units lies on a carpet up to 30 m thick of mylonite, phyllonite and cataclasite, formed mainly from rocks of the Alhamilla Unit (Platt 1982, Behrmann & Platt 1982). The lower carbonate unit (e) is

involved in the mylonitic deformation, but is probably part of the Aguilón nappe, as no dolostone occurs in the underlying Alhamilla Unit.

The sequence described above has a suggestive symmetry, and in this paper we present structural data demonstrating that the Aguilón nappe is a recumbent isoclinal fold. This allows us to suggest a pre-folding sequence, from bottom to top: black schist, phyllite and quartzite (PQ), carbonates. This sequence was not a simple conformable succession, however, as there is a marked difference in metamorphic grade between the black schist and the PQ, suggesting that the contact is either an unconformity or a fault. The age of the black schist is not known, but it is likely to be pre-Triassic.

The contact between the PQ and the carbonates is commonly a décollement surface, but there is no evidence for major translation along it. In an area of good structural control in the Bco Castillo (626887), cross-bedding in quartzite indicates that the PQ youngs towards the carbonates. The lower part of the latter is Middle Triassic, so the PQ is likely to be a Permo-Triassic red-bed sequence.

LARGE-SCALE STRUCTURE

The Aguilón nappe is warped around the Neogene anticlinorium of the Sierra Alhamilla, and on the north side of the Sierra it has been greatly disturbed by Neogene high-angle faults (Figs. 3–5). The overall geometry of the nappe can still be discerned on the cross-sections, however. Note that the PQ becomes much thinner northwards, and the black schist virtually disappears: only isolated outcrops a few tens of metres across are found on the north side. In the centre of the range (Risco del Aguilón, 572917; Colativí, 621948) the upper carbonate sequence comes within a few metres of the basal contact. There is no recognizable 'closure' of the fold-nappe: the existence of the structure being deduced from the symmetry of the lithological sequence and the pattern of small-scale structures in the PQ and black schist, discussed below. The lower limb has been

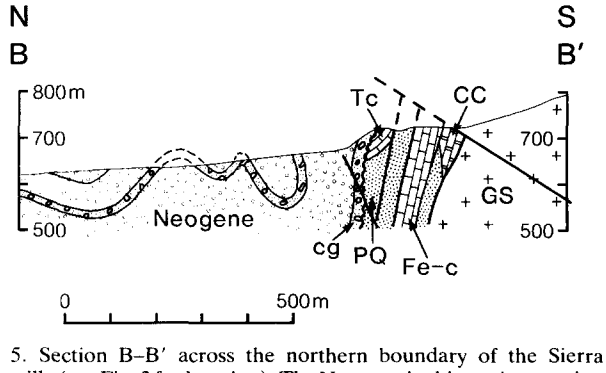

Fig. 5. Section B–B′ across the northern boundary of the Sierra Alhamilla (see Fig. 3 for location). The Neogene in this section consists of marls with calcarenite and rudite turbidite beds of Tortonian age (IGME 1973, geological map sheet Tabernas). cg, conglomerate; Tc, Triassic dolomite; PQ, multicoloured phyllite and quartzite; Fe-c, Iron-rich carbonate rocks; CC, cargneule and calc-mylonite with tectonic blocks of dolomite, phyllite, schist, and quartz–feldspar–tourmaline mylonite; GS, grey mica–schist.

greatly thinned and disrupted, so that the structural sequence described above is not everywhere complete. This modification is likely to have occurred during nappe transport.

In the northwest of the Sierra, the basal fault of the Savín Unit cuts down through the carbonate sequence of the Aguilón nappe, which is locally reduced to less than 1 m of mineralized dolomite breccia. A zone of calc-mylonite with a N–S elongation lineation is developed on the contact.

The Aguilón nappe appears to be larger than its present exposure in the Sierra Alhamilla (25 km E–W, 11 km N–S), but its total extent cannot be estimated. Similar Alpujarride sequences, including medium-grade black schist, are exposed in adjacent ranges—Sierra Cabrera (Westra 1969), Sierra Gador and Sierra de los Filabres (Vissers 1981)—but it naturally cannot be assumed that these form part of the same individual structure as the Aguilón fold-nappe.

SMALL-SCALE STRUCTURES

The PQ and black schist, in common with schistose rocks elsewhere in the Betic Zone, have a complicated small-scale structural geometry produced by the superposition of several sets of folds and foliations. The main reasons for describing these structures in some detail are: (1) because they demonstrate the existence of the fold-nappe, and determine its direction of closure; (2) they allow the metamorphic history to be related to nappe emplacement and (3) they allow some conclusions to be drawn about the rheology of the nappe. On the other hand, some of the structures developed are of local significance only, and we warn against the arbitrary correlation of the deformation sequences described here with those found elsewhere in the Betic Zone.

The longest and most complete section through the nappe is provided by the Rambla del Agua in the south centre of the range. This section will be described in some detail: the others briefly, to show to what extent they differ from or confirm the conclusions drawn from the Rambla del Agua section.

RAMBLA DEL AGUA SECTION

The section will be described from south to north; that is, from the top of the structure downwards. The principal features are shown on the structural map (Fig. 6) and cross-section (Fig. 7).

The upper limb

Main-phase (D_s) *structures.* In and around the southern part of the Rambla, quartzites of the PQ are thrown into a prominent series of 1–10 m N-vergent folds (Fig. 8a), with E–W axes and S-dipping axial planes. Cross-bedding in the quartzites demonstrates that the folds

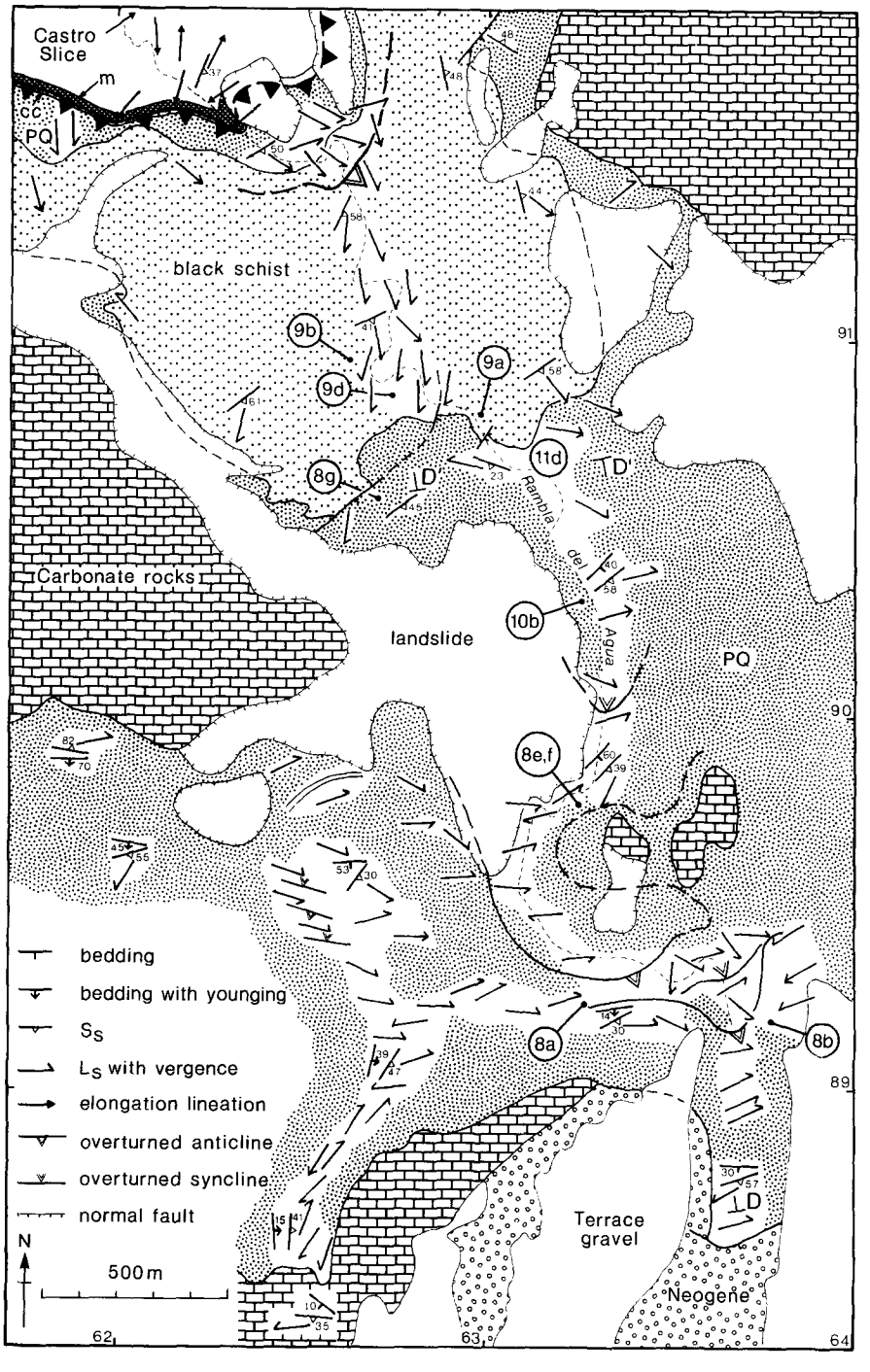

Fig. 6. Structural map of the Rambla del Agua area, southern Sierra Alhamilla. Only D_s structures are shown. PQ, phyllite–quartzite sequence; cc, calc–mylonite; m, ultramylonite. L_s lineations and minor fold axes are shown with the fold vergence or cleavage vergence direction indicated by the half-barb; e.g. a N-vergent fold has the half-barb on the north side of the arrow. Numbers in circles show locations of drawings and photographs (Figs. 8–11). Line of section in Fig. 7 is given by D and D'.

face upwards and to the north. An axial-plane cleavage (S_s) to these folds is well developed in the phyllites. The cleavage resembles a slaty cleavage in the field, but the metamorphic mica is coarser (10–20 μm) than in most slates. In quartzite there is a crude spaced cleavage (Fig. 10a) that anastomoses around detrital quartz (Fig. 10b). This intersects bedding to produce a pronounced E–W intersection lineation (L_s). Lineations and minor fold axes are shown on Fig. 6 with their sense of vergence. Fold vergence is used here simply as an indication of the sense of asymmetry, regardless of the orientation of the axial plane (Bell 1981, Weijermars 1983). 'Cleavage vergence' is used in the sense of Bell (1981) to indicate the sense of the bedding/cleavage relation.

We use the arbitrary letter subscript s for main-phase structures to avoid implying a fixed position in a temporal sequence, as this varies according to the previous history of the rocks.

Pre-main-phase structures (D_r). A foliation (S_r), defined by alternating 1–2 mm quartz-rich and mica + opaque-rich bands (Fig. 10c), is locally visible at a variable angle to bedding. It is refolded by D_s folds (Figs.

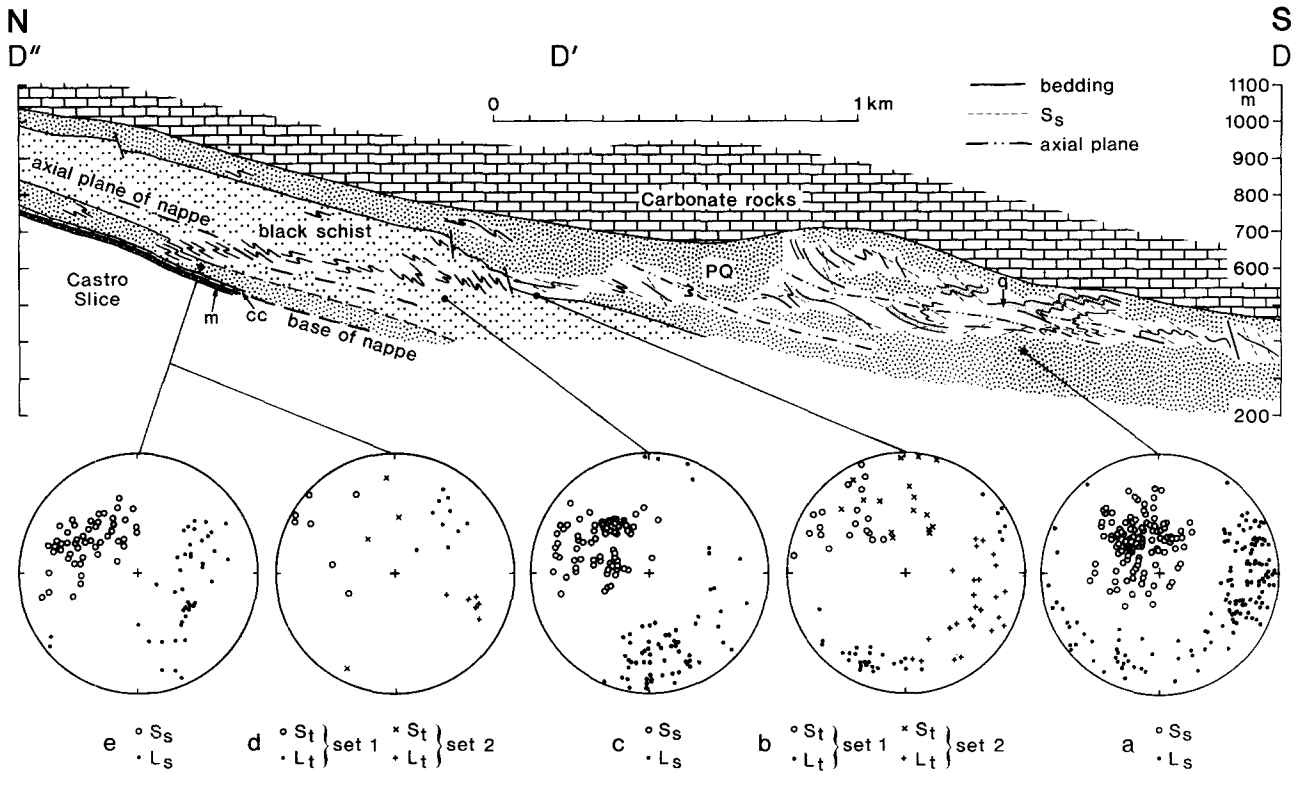

Fig. 7. Composite structural section D–D′–D″ along the Rambla del Agua (see Figs. 3 and 6 for location). Data have been projected in from either side; hence the lack of a topographic profile. q, quartzite. Other abbreviations as in Fig. 6. Only D_s minor structures are shown. Equal-area orientation plots: (a) D_s from the upper limb in PQ. (b) D_t from around the upper contact of the black schist. (c) D_s from the black schist. (d) D_t from the inverted limb. (e) D_s from the inverted limb in PQ. S_s & S_t, poles to foliation; L_s & L_t, intersection and crenulation lineations and minor fold axes. See text for the explanation of the two sets of D_t structures, and for discussion of fold-vergences in the black schist.

8b & c), and is axial planar in Rambla del Agua to a fold that is transected by S_s. S_r and S_s may alternate as the strongest fabric in adjacent beds of contrasting rock-type (Fig. 8d). No systematic sets of folds or lineations are preserved and the foliation cannot be traced continuously over a significant distance. The relation between S_r and bedding is only clearly observable in the south, where it is S-vergent (Figs. 8c & d).

Variation with depth. Main-phase folds and foliation can be traced northwards along the Rambla when traversing structurally downwards through the nappe. Continuous tracing in areas of good exposure is of the utmost importance in establishing their identity. Both style and orientation of D_s structures vary considerably with rock-type and with strain (Figs. 6–8), and S_s is not always the most prominent foliation.

Reversals in D_s fold and cleavage vergence reveal 100-m scale N-vergent folds. The use of vergence requires considerable care, as the trend of D_s fold axes and bedding–cleavage intersection lineations (Figs. 6 and 7) varies from SE (130°) through E to NE–SW. The more extreme deviations from the average E–W trend occur in phyllite, and particularly in the overturned limbs of the major folds, where the strain is highest. It is likely, therefore, to be caused by initial non-cylindricity of the folds, accentuated by rotation towards an elongation direction lying roughly N–S. No elongation lineation is developed at this level, however.

With depth in the section, D_s folds become tighter (Fig. 8), S_s becomes more intense, and sedimentary textures and structures are increasingly obscured. The post-buckling increment of D_s shortening strain in folded quartzite layers, estimated from fold profiles using the method of Milnes (1971), increases from 20 to 25% at the top of the PQ to 40% near the bottom. S_s takes on the appearance of a crenulation cleavage, with a spacing varying from 0.1 mm to several cms. A strong differentiation of quartz produced pronounced quartz-rich microlithons in the hinge zones of the crenulations that may resemble bedding (Figs. 8e & f and 11b & c). This change in character of S_s suggests that the pre-main-phase foliation S_r may also intensify with depth. S_r does in fact become more clearly visible as a penetrative fabric both in outcrop (Fig. 11b) and in thin section.

Near the contact with the underlying black schist, D_s folds become very tight, but are still clearly N-vergent (Fig. 8g). The angle between S_s and bedding becomes difficult to detect. S_r is largely obliterated, but S_s remains differentiated on a 1–2 mm scale suggesting that it originated as a crenulation cleavage.

Post-main-phase structures (D_t). Crenulations and metre-scale folds with steep to vertical axial planes locally overprint S_s (Fig. 8g). NW- and NE-trending sets are developed, both of which are N-vergent, and are spatially associated with faults and a zone of steep dips that brings the black schist to the surface. Overprinting relations between the two sets are not developed, and they are grouped here as D_t to indicate that they postdate D_s. A locally intense differentiated crenulation cleavage S_t is developed (Figs. 11d and 12a).

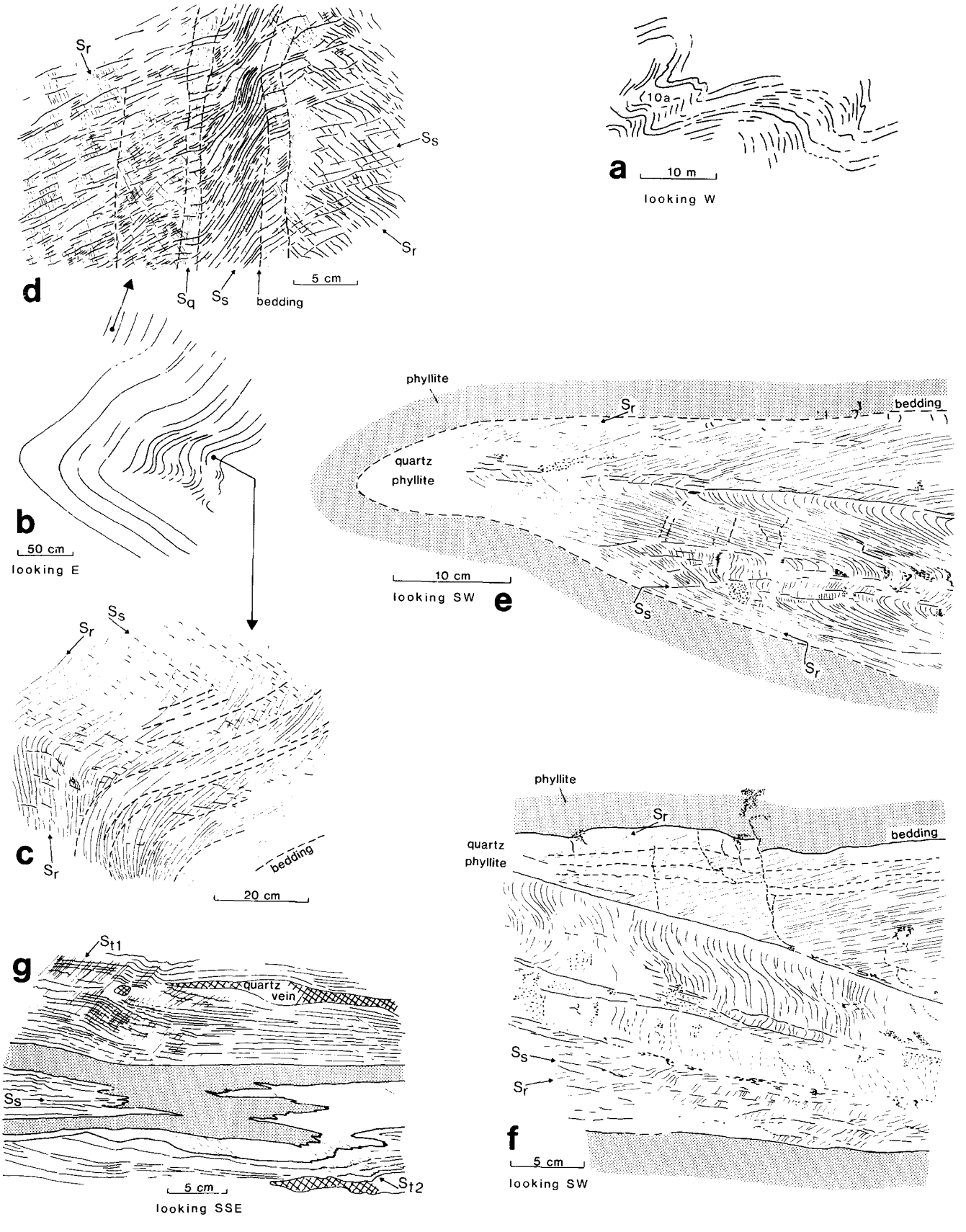

Fig. 8. Sketches in profile of structures in the upper limb PQ. See Fig. 6 for locations. (a) N-vergent D_s folds in quartzite (stippled) and quartz phyllite. (b) Hinge of a D_s fold in quartz phyllite with locations of parts (c) and (d) of this figure. (c) Independent folding of bedding and S_r. S_r is the dominant foliation, S_s is weak. See Fig. 10(d). (d) Interplay of S_r and S_s in beds of varying composition. S_r dominates in more quartz-rich layers, S_s in more micaceous layers. S_q is a bedding-parallel fabric, possibly sedimentary lamination. See Fig. 10(a). Note refraction of S_s in the more micaceous central layer. (e) Tight D_s fold with large-scale crenulations of S_r. S_r is oblique to bedding and has been independently folded. See Fig. 11(b). (f) Large-scale differentiated D_s crenulations, developed by folding of oblique S_r independently of bedding. See Fig. 11(c). (g) Isoclinal NE-vergent D_s fold near the lower contact of the upper limb PQ, overprinted by a NW-vergent and a NE-vergent set of D_t crenulations.

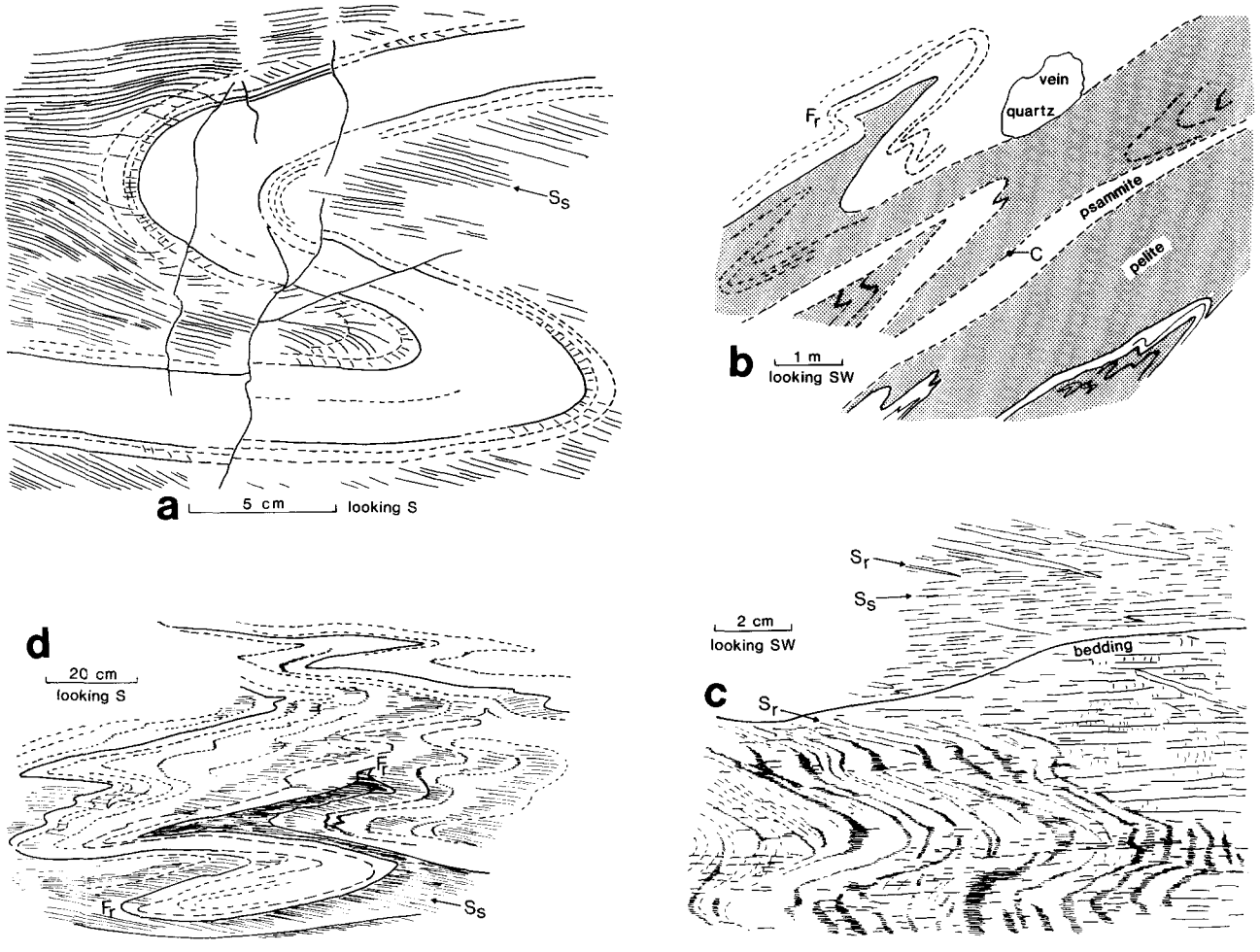

Fig. 9. Sketches in profile of structures in the black schist. See Fig. 6 for locations. (a) E-vergent flattened buckle fold in quartz-rich layer in psammitic schist. The trajectories of the crenulation cleavage, S_s, resemble those predicted by Dieterich (1969) for finite-strain axes around folds of this type. (b) 10-m scale W-vergent D_s folds in the overturned limb of a 100-m scale fold (see Fig. 7). Note small D_r fold (shown Fr) at top left. (c) Detail of cleavage pattern in psammitic and pelitic schist: see (b) for location. The irregular bedding surface is probably a primary sedimentary feature, and causes a local anomaly in the S_s cleavage-vergence, which is westwards elsewhere in this layer. (d) D_r/D_s fold interference. Figure 12(b) is a close-up of the central part of this sketch, and Fig. 13(b) of the refolded D_r fold at the bottom.

The core of the nappe

The core of the nappe is occupied by a body of medium-grade black graphitic mica-schist. The upper contact is obscured by a young steep fault in the floor of the Rambla del Agua, but elsewhere it is undisturbed and roughly parallel to the main-phase schistosity (S_s). S_s can be traced across the contact between the PQ and the black schist, and is the dominant fabric in both rock-types. In the black schist, S_s is differentiated into 1–2 mm thick quartz-rich and mica-rich bands (Figs. 12b & c), and was formed by crenulation of an earlier schistosity defined by coarse (200 μm) mica (Fig. 12d). Even in outcrop, S_s can be seen to wrap around, and hence post-date, the large porphyroblasts of garnet and staurolite.

10 cm–1 m asymmetric folds are common in psammitic layers: most of these are D_s folds, with S_s developed as an axial-plane foliation (Figs. 9a and 12b). These folds and associated intersection lineations plunge consistently south in the schist, approximately at right angles to the average trend in the PQ (Fig. 7). This might be caused by rotation of the folds during progressive strain, or by superposition of D_s strain on differently oriented layering in PQ and black schist. The strain in the black schist is higher than in the PQ (minimum estimates from D_s fold profiles lie in the range 30–55% shortening) but there is no abrupt increase in strain corresponding to the abrupt change in orientation across the contact. The difference is most likely to be due to a difference in orientation of the layering prior to D_s. This is a reasonable supposition, as the contact must represent some type of pre-D_s discontinuity, in view of the change in metamorphic grade across it.

The difference in fold trend between the PQ and the black schist causes difficulty in interpreting the vergences. The dominant vergence near the upper contact is E, which suggests that E-vergences in the schist have the same significance, in relation to major structures, as N-vergences in the PQ. The fold trend locally swings from S, through SE, to E (Figs. 6 and 7), which tends to confirm this. On the cross-section (Fig. 7), which is roughly parallel to D_s folds in the black-schist, E-vergences have therefore been shown as N, and W-vergences as S. Note that in adjacent sections through the black schist (see below), D_s folds trend SE or E, and are N-vergent near the top of the body (Fig. 14).

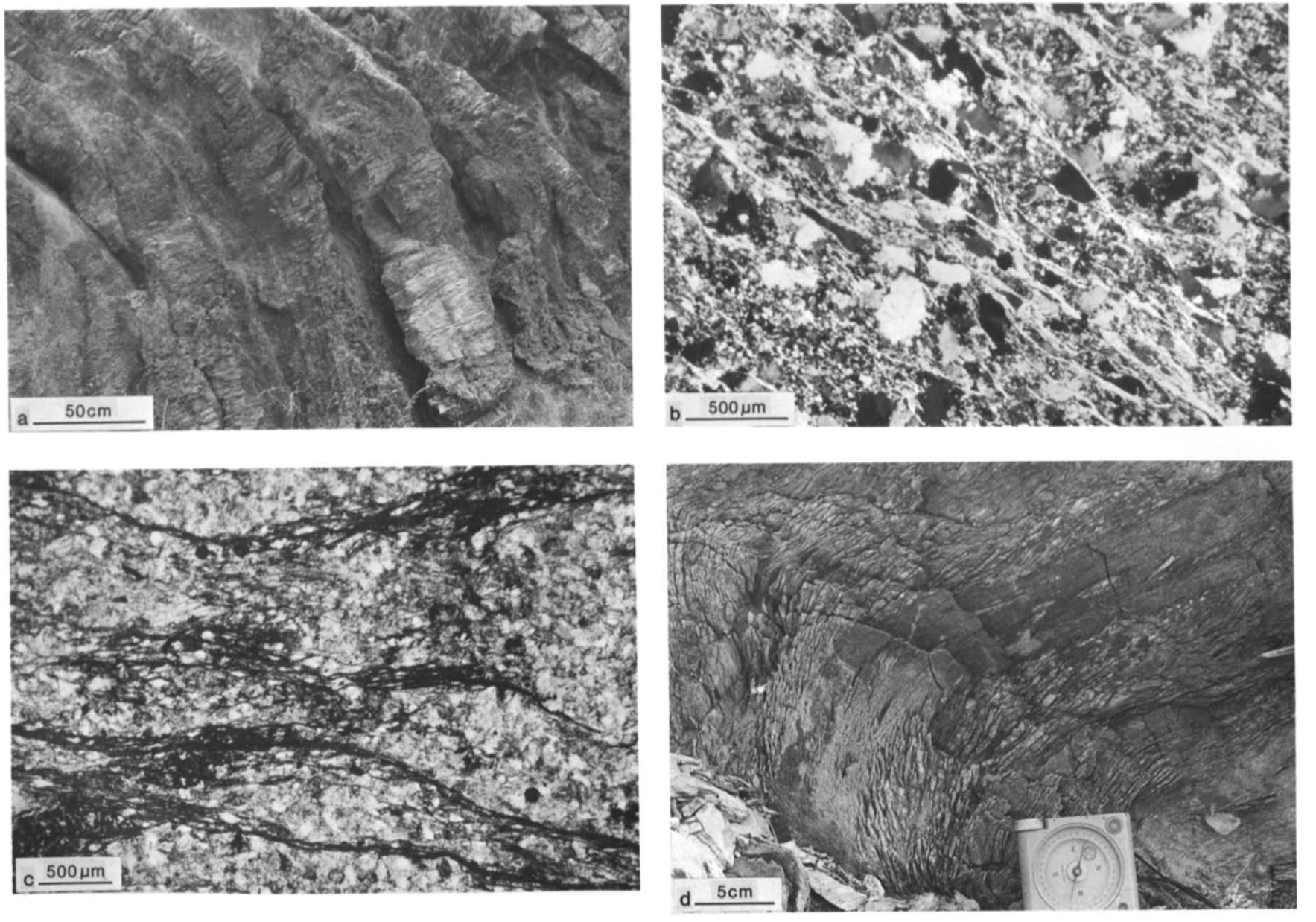

Fig. 10. (a) Spaced cleavage, S_s, in quartzite from the hinge of a D_s fold, upper limb PQ. See Fig. 8(a) for location. Looking west. (b) Photomicrograph of S_s rough cleavage anastomosing around detrital quartz grains in quartzose phyllite. Note flat edges of quartz grains truncated by pressure solution adjacent to white mica. See Fig. 6 for location. (c) Photomicrograph of domainal S_s cleavage in phyllite (nearly horizontal) cutting across broad S_r differentiation band rich in white mica and opaque minerals (top-right to bottom-left). Bedding (not visible) is horizontal. Location as for Fig. 8(b). (d) Minor D_s fold in quartz phyllite with refolded S_r and weak S_s. See Fig. 8(c) for sketch and location. Looking east.

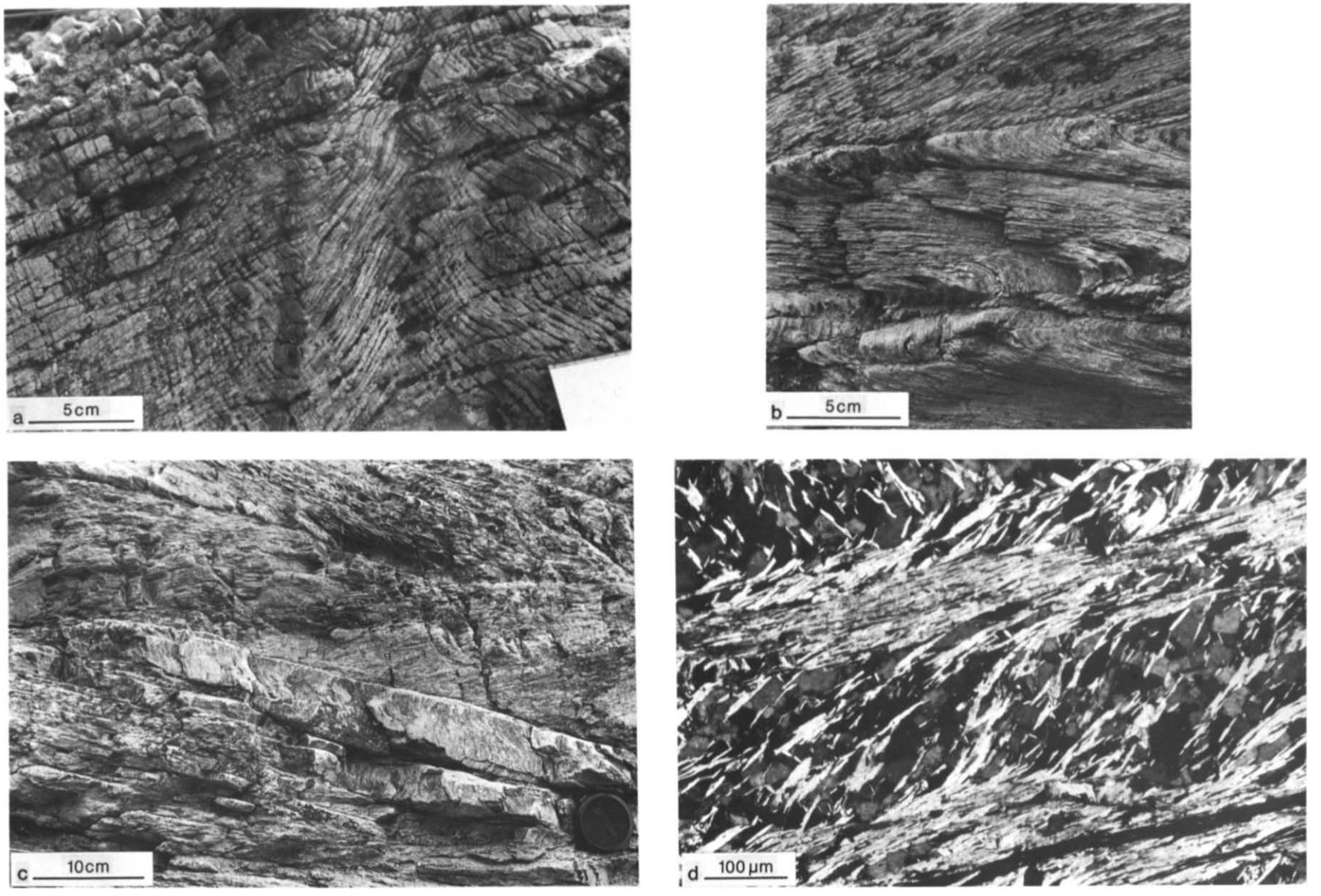

Fig. 11. (a) S_r (dipping right) and S_s (dipping left and refracted) in vertical beds of quartz phyllite. See Fig. 8(d) for sketch and location. Looking east. (b) Large-scale crenulation of S_r in quartz phyllite producing broad differentiation bands that define S_s. See Fig. 8(e) for sketch and location. Looking southwest. (c) Massive quartz-rich differentiation bands parallel to S_s, produced by crenulation of S_r (dipping left). Bedding, faintly visible in centre of photograph, is horizontal. See Fig. 8(f) for sketch and location. Looking southwest. (d) Photomicrograph of S_t differentiated crenulation cleavage in phyllite. See Fig. 6 for location.

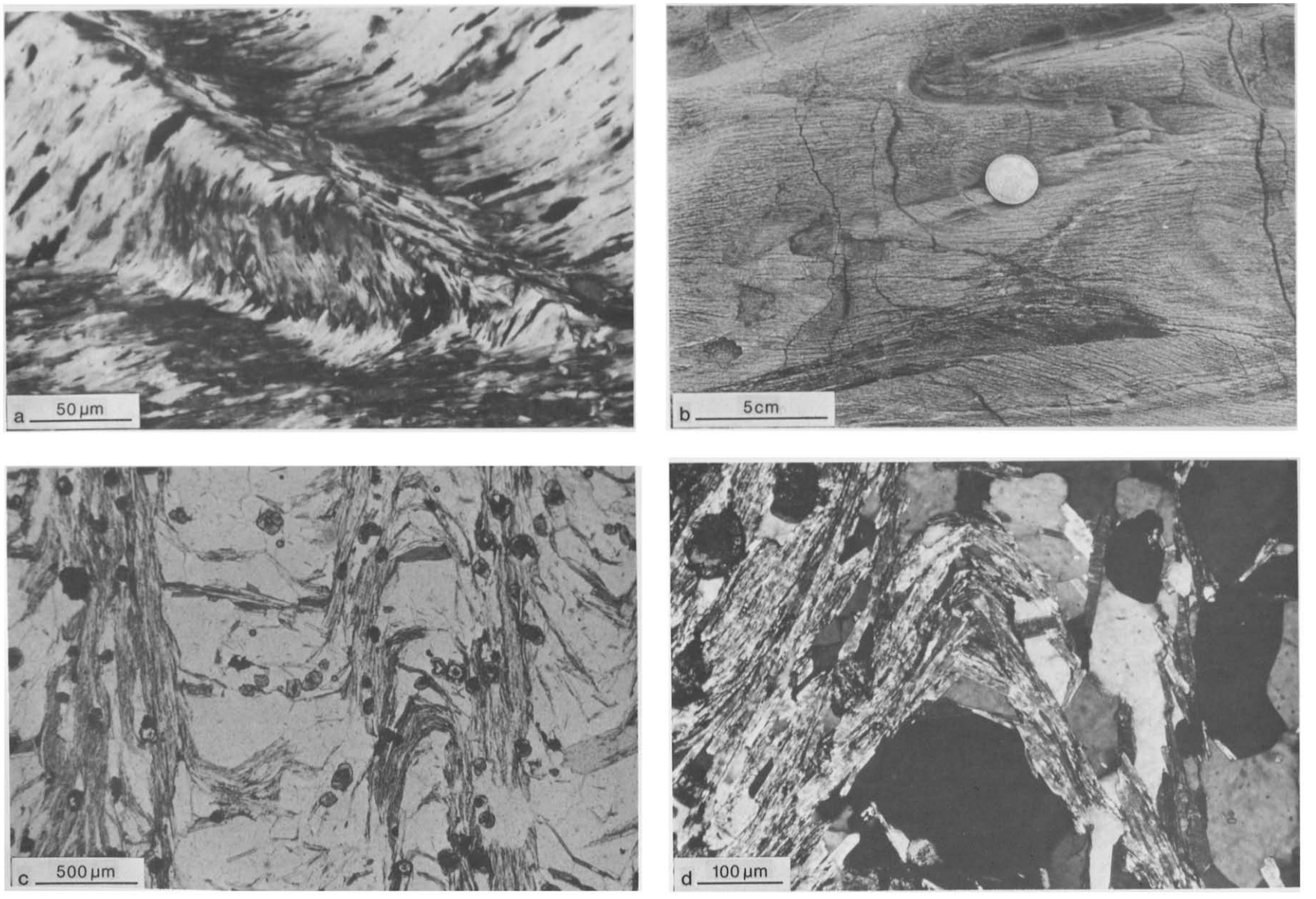

Fig. 12. (a) Photomicrograph of D_1 crenulations in pure mica phyllite. See Fig. 6 for location. (b) E-vergent D_s folds in semi-pelitic schist from the black schist body. Note the broadly spaced S_s differentiated crenulation cleavage. See Fig. 8(d) for location. Looking south. (c) Photomicrograph of S_s crenulation cleavage in black pelitic schist. Note strong differentiation of quartz into crenulation hinges. Small porphyroblasts are garnet. Location as for Fig. 9(a). (d) Photomicrograph of a D_s crenulation hinge from the black schist shown in (c).

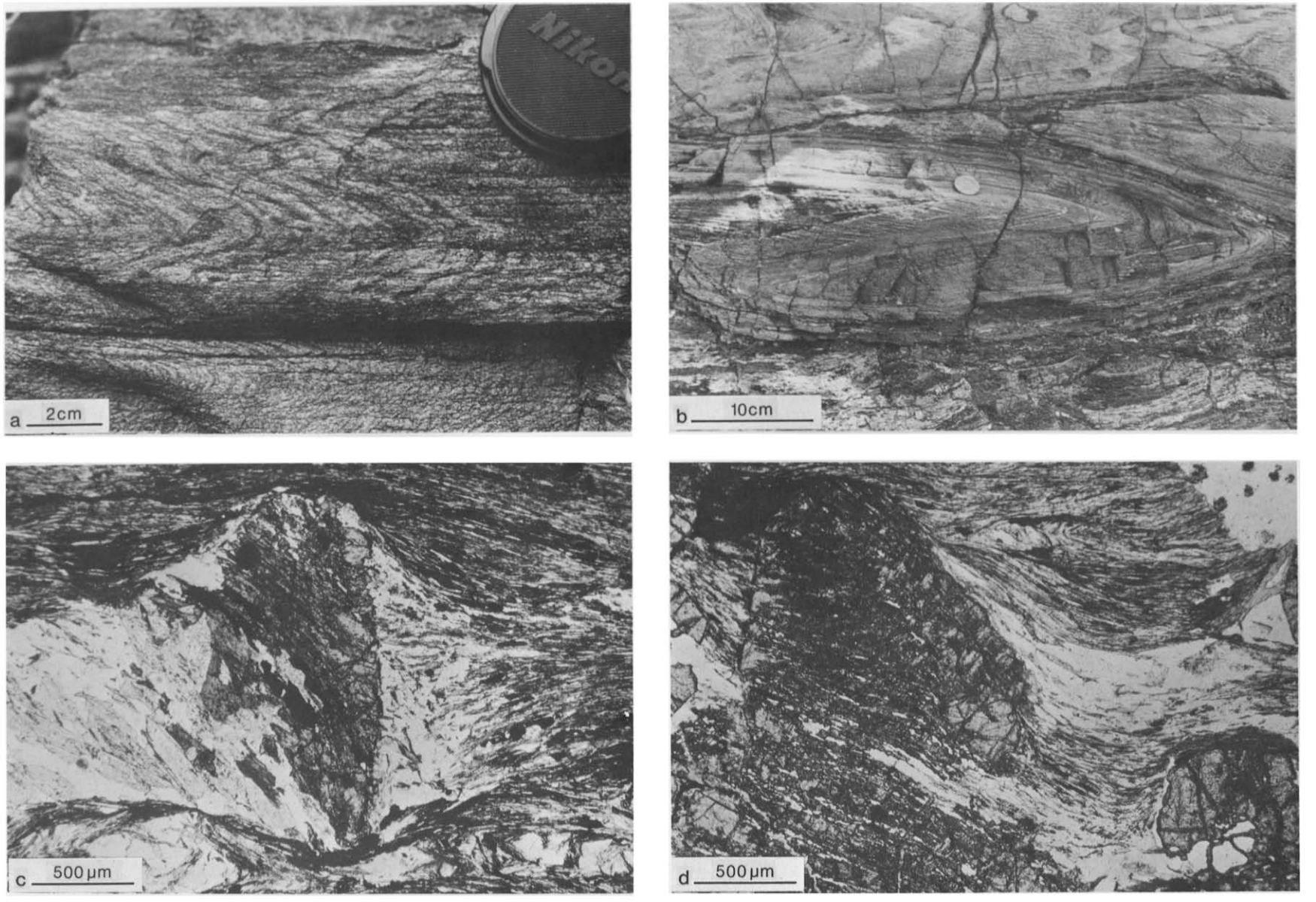

Fig. 13. (a) Independent folding of broadly differentiated S_r foliation in unfolded bedding. Irregular bedding surface between black pelitic and psammitic schist is visible at top of photograph. Strong crenulation cleavage, S_s, is horizontal. See Fig. 9(b) for context and 9(c) for sketch. Looking southwest. (b) Refolded D_r fold in black semi-pelitic schist. See Fig. 9(d) for location. Looking south. (c) Photomicrograph of porphyroblast in black pelitic schist. S_s (horizontal) wraps around the crystal, leaving quartz-filled deformation shadow either side, and truncates the internal fabric (S_r) in the crystal. Location as for Fig. 9(b). (d) Photomicrograph of staurolite in black schist. The internal fabric (S_r) can be traced across the grain margin into a fabric which is tightly crenulated (top right) to produce S_s (horizontal). Porphyroblast at bottom right is garnet.

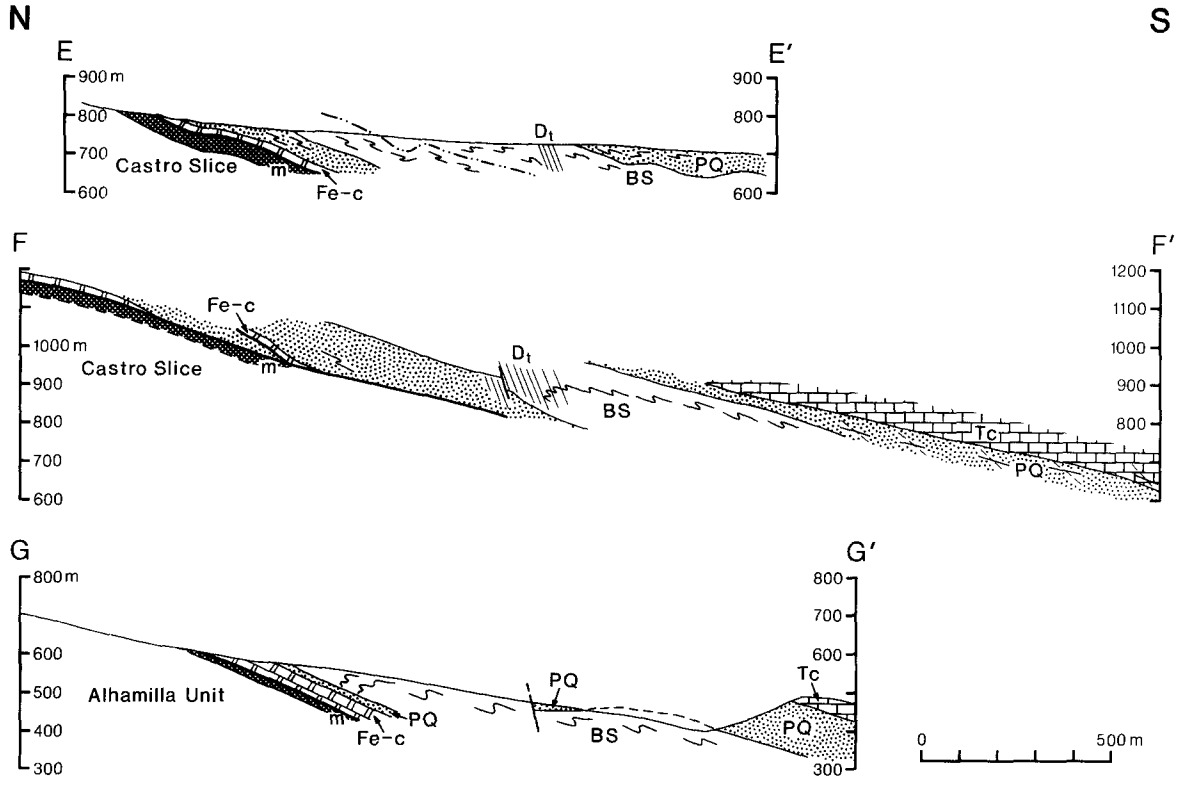

Fig. 14. Sections across the Aguilón nappe. See Fig. 3 for locations. E–E', Rambla de Inox; F–F', Barranco Martínez; G–G', Barranco Infierno-Barranco de Pajonares. Abbreviations as in Figs. 5 and 6.

The vergence of small-scale D_s folds is commonly variable in individual outcrops, indicating the presence of folds on a 10–100 m scale (Figs. 7 and 9b). The overall geometry of these larger folds was unravelled where possible, and the vergence shown on the map and section. Otherwise, minor folds were counted over 50 m of section, and the majority vergence direction used. The data show that E-vergent folds are dominant through most of the section. 50 m structurally above the base of the body, however, the vergence reverses to W. This suggests that the black schist constitutes an E-closing fold, with a very thin lower limb (Fig. 7).

Pre-main-phase folds and foliation are locally visible in the schist. These are referred to as D_r, but it is not implied that they are necessarily coeval to or related to D_r in the PQ. S_r is locally visible in psammitic schist; it may be parallel or oblique to the lithological layering, and may be folded independently of the layering (Fig. 9c). Pre-D_s folds (Fig. 9d) may be related. S_r is a differentiated crenulation cleavage, and a pre-S_r schistosity is visible in the microfold hinges.

Post-main-phase folds and crenulations are well developed around the main D_s axial zone, and extend downwards across the lower boundary of the black schist. Axes trend E–W, axial planes and crenulation cleavage dip steeply N. Locally, three foliations (S_r, S_s and S_t), all oblique to layering, are visible in outcrop.

The lower limb

The lower contact of the black schist has locally been disturbed by minor faulting, but the principal foliation is S_s, and this can be traced across the contact into the underlying phyllite. The contact is locally oblique to S_s, and is affected by SW-vergent D_s folds on a scale of 1–3 m. D_s folds above and below the contact trend SE and are SW-vergent. Tight D_s folds are common in the PQ below the contact, and the majority are S-vergent (Figs. 6 and 7). This clearly indicates that the lower unit of PQ forms the overturned limb of a major N-closing isoclinal D_s fold.

Near the lower contact irregular sets of kinks, and locally a horizontal extensional crenulation cleavage (Platt & Vissers 1980), are developed. The lower contact of the nappe is marked by 0.5 m of foliated carbonate rock, which overlies intensely foliated mylonite and mylonitic schist of the Alhamilla Unit. The latter have a pronounced stretching lineation that plunges on a bearing of 235° in the mylonite, and 200° in the underlying schist (Figs. 3 and 6).

COMPARATIVE SECTIONS ACROSS THE NAPPE

The other structural sections across the Aguilón nappe provide an insight into the lateral continuity of the structures described above. We are cautious about the correlation of sets of small-scale structures however, as in the absence of continuous exposure we believe the only reliable criterion is a demonstrated relation to the major structure.

East of the Rambla del Agua, in the Rambla del Inox (Fig. 14, section E–E'), the same symmetrical sequence

of rock types occurs. The most prominent set of folds in both the PQ and the black schist trends SE and change from NE to SW vergent within the black schist. This suggests that they are D_s structures, related to the fold-nappe and demonstrating its continuity eastwards. They are locally overprinted by N-vergent folds and (in the PQ) by a steep crenulation cleavage.

West of the Rambla del Agua, in the Barranco Martínez (Fig. 14, section FF'), D_s folds are variable in trend, but there appears to be a change in vergence between the upper and lower limb PQ. The axial zone in the black schist, however, is strongly overprinted by post-main-phase minor folds and crenulation cleavage. The lower limb of the nappe appears to be imbricated: the lower PQ is exceptionally thick and the lower carbonate unit is repeated.

Further west, in the Barranco del Infierno (G–G'), the lower PQ is reduced to less than 10 m. It overlies a continuous band of mineralized dolomite breccia, which in turn rests on the mylonitic carpet at the base of the nappe. Three sets of small-scale folds are present in the black schist: all trend roughly E and are N-vergent. The middle set, however, becomes symmetrical in the lowest 20 m of the black schist, and this set may be D_s. If so, the S-vergent lower limb has been excised. Except in the symmetrical zone, D_s structures are not the most prominent: small N-vergent flattened buckle folds are only locally developed, associated with a 0.5 cm spaced differentiated crenulation cleavage in pelitic schist. In more quartzose rocks, a pre-D_s schistosity associated with tight to isoclinal folds is well developed. Open to tight post-D_s folds and crenulations are developed everywhere.

From east to west across the area depicted in Fig. 3, there appears to be a decrease in intensity of D_s. This may be related to the disappearance westward of the lower limb and axial zone of the fold-nappe. The N-vergent post-D_s structures intensify westwards. These probably formed during nappe emplacement because they have no obvious equivalents in the underlying Alhamilla Unit (Platt & Behrmann in prep.). They may be related to the local disruption of the fold-nappe structure.

Structures in the carbonate rocks

Around Mina (663945) the carbonate rocks are cut by a set of low-angle reverse faults (Fig. 15). Their geometry suggests imbrication by southward thrusting along a décollement surface at the base of the carbonate sequence. The PQ below is not involved in the thrusting, but the contact is largely obscured. These S-directed thrusts, and some 100–300 m scale S-vergent folds in the carbonate rocks in the south and west of the Sierra, are not easily reconciled with the N-vergent D_s and D_t structures in the PQ and black schist, but we have no basis for establishing their relative age.

METAMORPHIC HISTORY

The Aguilón nappe comprises two metamorphic units: the black schist, of medium grade, and the PQ and carbonate sequences, of low grade. These two units were probably juxtaposed during or immediately before D_s (see below).

Black schist

The medium-grade assemblage in black pelitic schist in the Rambla del Agua is quartz + muscovite + biotite + garnet + staurolite ± albite. Aluminium silicate minerals have not been recorded from the area shown in Fig. 3. Graphite, tourmaline, apatite, rutile and magnetite are minor phases. The assemblage indicates a peak temperature in the range 540–600°C (Hoschek 1969, Rao & Johannes 1979). This assemblage clearly predates the principal foliation (S_s), which wraps around the porphyroblasts, leaving quartz-filled deformation shadows on either side, and truncates straight trails of inclusions in the staurolite (Fig. 13c). These inclusion trails, which are defined by quartz and graphitic dust, can locally be traced across the crystal boundaries into the mica schistosity (S_r) that is crenulated to form S_s (Fig. 13d). The metamorphic peak, as represented by staurolite, therefore occurred between D_r and D_s. The inclusion trails at the margins of some staurolite grains are curved or folded indicating some deformation (presumably the beginning of D_s) during their growth. Garnet is included in staurolite, and contains curved inclusion trails, so it may have grown during D_r.

During D_s the schistosity, S_r, defined by oriented biotite and muscovite, was strongly crenulated and transposed. Muscovite partly recrystallized in crenulation hinges, by grain-boundary migration on a scale of

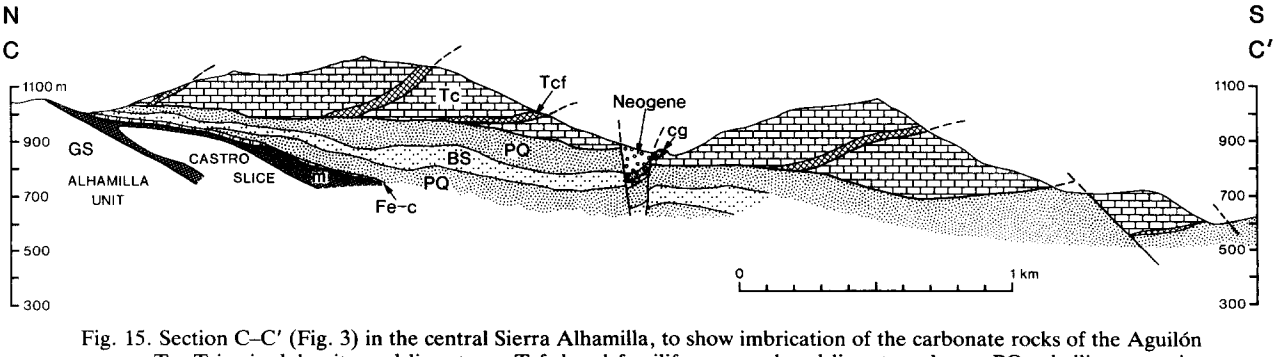

Fig. 15. Section C–C' (Fig. 3) in the central Sierra Alhamilla, to show imbrication of the carbonate rocks of the Aguilón nappe. Tc, Triassic dolomite and limestone; Tcf, basal fossiliferous marl and limestone layer; PQ, phyllite–quartzite sequence; BS, graphitic mica schist with garnet and staurolite; Fe-c, Iron-rich carbonate rock; m, mylonite and ultramylonite; GS, grey mica schist.

about 50 μm, to relieve lattice strain (Fig. 12d). Biotite was largely altered to chlorite. Both garnet and staurolite underwent some retrogressive alteration to chlorite and white mica: this was most extensive near the upper and lower boundaries of the black schist body, possibly because of the availability of an external source of water. Quartz was extensively remobilized by a solution-transfer mechanism to produce the differentiated foliation S_s. D_s therefore appears to have occurred under greenschist-facies conditions: the instability of biotite in favour of chlorite suggests a temperature below 450°C. These conditions persisted after D_s: porphyroblasts of chlorite, albite and locally chloritoid grew over S_s helicitically. During D_t, quartz was still mobile (solution transfer), but recrystallization of mica was very limited. These relationships are summarized in the table below.

D_t	chlorite	solution transfer of quartz
Static	chlorite, albite, chloritoid	
D_s	chlorite, albite	solution transfer of quartz and recrystallization of white mica
Static	staurolite, albite, muscovite	
D_r	garnet, biotite(?)	

PQ

The main assemblage in the phyllite is quartz + white mica + chlorite + carbonate minerals + magnetite. Chloritoid, albite, and epidote are locally present. Accessories include tourmaline, apatite, and zircon. The assemblage is characteristic of the greenschist facies, and the absence of biotite suggests that the peak metamorphic temperature did not exceed 450°C. There is no evidence in either the lower or upper limb PQ for an early medium-grade event, as found in the black schist; and the preservation of clastic textures (Fig. 10b) argues against such an event. Crystallization or recrystallization of quartz, white mica, and chlorite occurred during both D_r and D_s. During D_t, quartz was mobilized by solution-transfer (Fig. 11d), but grain-boundary migration of mica in crenulation hinges was limited to a scale of less than 10 μm (Fig. 12a), suggesting lower temperatures than during D_s (compare Fig. 12d).

PQ–black schist contact

The change in peak metamorphic grade between the PQ and the black schist appears to be abrupt. Garnet is present in the black schist at both upper and lower contacts. Staurolite appears within about 30 m structural distance of the upper and lower contacts. Its absence at the contacts is probably due to more advanced retrogressive metamorphism there. The peak conditions of metamorphism in the two bodies cannot be constrained precisely, but the temperature difference must have been at least 100°C, and may have been as much as 200°C. The contact is therefore a marked discontinuity: either a fault or an unconformity that was subsequently folded around the nappe.

The black schist is probably pre-Triassic, so there is a possibility that it has experienced a Hercynian metamorphism. This was suggested for supposedly Palaeozoic rocks in the Alpujarride complex by Egeler & Simon (1969), and a pre-Triassic metamorphism produced andalusite and biotite in some Nevado-Filabride rocks (Diaz de Federico *et al.* 1978).

If the contact is a Permo-Triassic unconformity, D_r in the black schist (which predates the staurolite) must be a pre-Triassic event. D_r in the PQ then presents a problem, as this must be post-Triassic, yet would have no equivalent in the black schist. This somewhat circumstantial argument suggests that the amphibolite-facies metamorphism in the black schist is post-Triassic, and that the contact is a fault that juxtaposed the two units after D_r, and either before or early in D_s. The metamorphic evidence is consistent with the two units having been together during and after D_s, and hence during formation of the fold-nappe.

More cogent evidence for a post-Triassic age for the metamorphism of the black schist comes from elsewhere in the Betic Zone. Amphibolite-facies metamorphism affects both Permo-Triassic sediments and pre-Triassic graphitic schist of the Alpujarride complex in the Sierra de las Estancias (Akkerman *et al.* 1980), Sierra Almijara (Torres-Roldán 1974) and Serrania de Ronda (Loomis 1972, Westerhof 1977).

If the contact between black schist and PQ is a pre- or syn-D_s fault, it has excised part of the original metamorphic zonation. Assuming, for the sake of argument, that the original isograds were horizontal, and related to a geothermal gradient of 30°C km (appropriate to a Barrovian metamorphic facies series), then the fault is an extensional (normal) fault that has cut out over 3 km of rock.

DISCUSSION AND CONCLUSIONS

Structural evidence for a fold-nappe

The existence of a major recumbent fold, suggested by the symmetrical distribution of rock-types in the nappe, is confirmed by the reversal in the sense of asymmetry of D_s folds in the Agua and Inox sections. The overturned limb lies directly on mylonite of the Alhamilla Unit, so the structure is a fold-nappe in the sense of Heim (1919): that is a major recumbent fold that has been thrust along its overturned limb.

No closure to the fold is exposed in the Sierra Alhamilla, and it must lie outside the range. The sense of closure may be indicated approximately by the minor D_s folds, but we must be sure that these have not been rotated towards the X-direction of strain during progressive deformation. Where D_s strain is weakest (in quartzite near the top of the PQ) the folds are E–W, and this is likely to have been their initial orientation. The only indication of the maximum elongation direction comes from the tectonites below the nappe, which have N- to NE-trending elongation lineations. Folds in the nappe locally deviate towards this direction, and it is

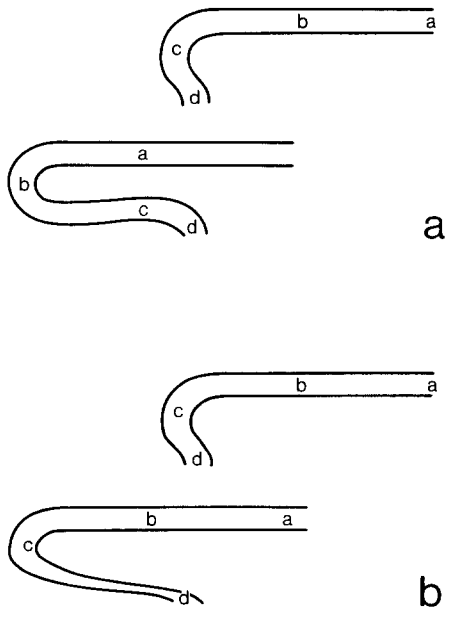

Fig. 16. Schematic sections to illustrate alternative ways of making a fold nappe. In (a), successive material-points (a to d) roll through the hinge and onto the lower limb. In (b), the hinge is fixed, and the lower limb is attenuated and inverted by shear.

reasonable to conclude that the E–W folds have been least affected by progressive strain. The nappe is therefore likely to have a roughly E–W axis, and to close northwards.

It is not entirely clear how a fold-nappe forms. There are two alternatives.

(1) As the nappe moves forward, the fold-hinge migrates through the material. The movement picture is that of a bulldozer laying track (Fig. 16a). The overturned limb need not be greatly thinned, but will suffer a polyphase deformation history as it is flexed into the hinge area, and then straightened again.

(2) The lower limb constitutes a ductile shear zone allowing forward translation of the upper limb (Fig. 16b). Rotation of the layering is largely a passive response to the shear strain. The lower limb will be greatly thinned, but nappe-related deformation is likely to be simpler than in the first model.

The Aguilón nappe has a greatly thinned lower limb, and there is no evidence for a downward increase in the complexity of deformation. It seems likely, therefore, that the overturned limb was rotated and inverted by shear, as suggested for the Morcles nappe by Ramsay (1981).

Either method of nappe formation requires a substantial component of motion (relative to the substrate) normal to the fold hinge line, in the direction of fold closure. The Aguilón nappe must therefore have been emplaced in a roughly northward direction. This conclusion has been independently confirmed by study of the footwall tectonites. These show a pronounced NNE–SSW trending stretching lineation, suggesting relative motion in this direction; and asymmetric quartz *c*-axis fabrics in these rocks suggest a northerly sense of shear (Behrmann & Platt 1982).

Creep mechanisms during nappe formation

Nappe movement was to a considerable extent accommodated by ductile deformation in the PQ and black schist, so it is important to consider the rheological state of these rocks. S_s in both units is a differentiated crenulation cleavage, defined by alternating micaceous cleavage zones and quartz-rich microlithons. Deformation occurs by flexural-slip microfolding of an earlier foliation. Microfold hinges are dilatant for geometrical reasons, and silica migrates by intergranular diffusion (pressure solution) from the limbs to the hinges (Cosgrove 1976, Fletcher 1977). Once the microfolds are initiated the diffusion of silica will control the rate of deformation, and hence the bulk rheology. Available theoretical and experimental evidence indicates that this type of volatile-assisted diffusional creep will obey an approximately linear viscous flow-law (Rutter 1976). At low rates of strain, it is therefore likely to be able to proceed at stresses lower than those required for creep mechanisms involving intracrystalline (dislocation) deformation, which obey power-law or elastic–plastic flow laws.

The PQ and black schist appear to have deformed by pressure-solution throughout their polyphase deformational history. S_r in the PQ is a spaced cleavage showing evidence of differentiation (Fig. 10c); S_r in the black schist (not necessarily related) is differentiated (Fig. 13a), and S_t in both units is a differentiated crenulation cleavage (Figs. 11d and 12a). In each case, the marked chemical differentiation must reflect extensive diffusion. At the temperatures prevailing during deformation, it is likely that this could only occur with the assistance of a volatile phase, probably water.

Mechanism of nappe emplacement

The structural history of the Aguilón nappe allows some tentative deductions about the mechanical processes of its emplacement. The dominance of solution-transfer processes in the schist and phyllite units suggests that emplacement occurred relatively slowly and under low deviatoric stresses: of the order of tens rather than hundreds of bars (Rutter 1976). The progressive downward increase in the D_s increment of strain through the nappe continues into the underlying mylonitic schists of the Castro slice, and is coupled with a change to the relatively high-stress deformation mechanism of dislocation creep at the lower boundary of the nappe. As argued by Platt (1982) this downward increase in both stress, strain, and presumably rate of deformation, in rocks of roughly similar mechanical properties, is not easily reconciled with a model of nappe emplacement by an external driving force (Chapple 1978). Such a model requires that stress be transmitted through a relatively strong medium that does not deform much, and that the strain be concentrated in weak zones where stress is relieved (Casey 1980). The concurrent downward increase in stress and strain in and below the Aguilón nappe, however, requires that the stress be continuously

maintained, probably by gravitational body forces. This downward increase of stress is consistent with the model of gravity spreading (Bucher 1956, Price 1973, Elliott 1976), which is a process of macroscopically ductile lateral flow under the stresses induced by a surface slope. The horizontal shear stress at depth h is given by $\rho g h \alpha$, where α is the surface slope.

The Aguilón nappe probably moved under an overburden of 10–15 km needed to cause the syn-D_s greenschist-facies metamorphism. At this depth, a regional surface slope of 3° would produce shear stresses in the range 120–160 bars, which is sufficient to drive the low stress deformational processes that operated in the nappe. Note that this depth is greater than any conceivable surface relief, so that gravity-sliding is ruled out as a process.

A requirement of gravity spreading is that a major part of the complex undergoes horizontal extension. Compressional deformation may occur at the leading edge of the complex, but the overall deformation is a lateral extension of the ductile rock-body. Major extensional structures are not commonly reported from orogenic belts, and the overwhelming evidence for crustal shortening in mountain belts suggests that gravity spreading can at best be a secondary process, consequent upon a phase of crustal shortening and thickening, which produces surface elevations and surface slopes (Price 1981). The probable presence of a post-metamorphic extensional fault between the black schist and the PQ, now folded around the Aguilón nappe, is therefore of considerable significance: nappe emplacement was apparently preceded by large-scale extension. A possible way in which the two events could have been related in a continuous process driven by gravity is suggested in Figs. 17 and 18.

Emplacement of the Higher Betic nappes by a gravitational process during the late stages of a metamorphic event has been suggested by Torres-Roldán (1979) and Platt (1982), and is supported in an intriguing way by the metamorphic evolution. Relatively early formed garnet–staurolite–kyanite assemblages were succeeded by cordierite + andalusite in Alpujarride rocks of the Sierra de las Estancias (Akkerman *et al.* 1980), by andalusite and then sillimanite + K-feldspar in the Sierra Cabrera (Westra 1969) and Sierra Almijara (Torres-Roldán 1974), and by andalusite followed by sillimanite + cordierite + K-feldspar in the Serranía de Ronda (Loomis 1972, Westerhof 1977). These histories indicate decreasing pressure accompanied by constant or rising temperature, which in each case occurred during and fairly late in the tectonic history. Rapid uplift and denudation during metamorphism is implied. This occurred before or during nappe emplacement, as the nappe contacts commonly postdate the peak of metamorphism (Egeler & Simon 1969). There is an abrupt increase in metamorphic grade downward across some of these contacts (e.g. that between Malaguide and Alpujarride), suggesting the presence of extensional faults similar to that between the black schist and PQ in the Aguilón nappe. The evidence is consistent with nappe emplacement having been caused by gravitational flow from an uplifted area of high heat-flow in what is now the Alborán Sea (Torres-Roldán 1979).

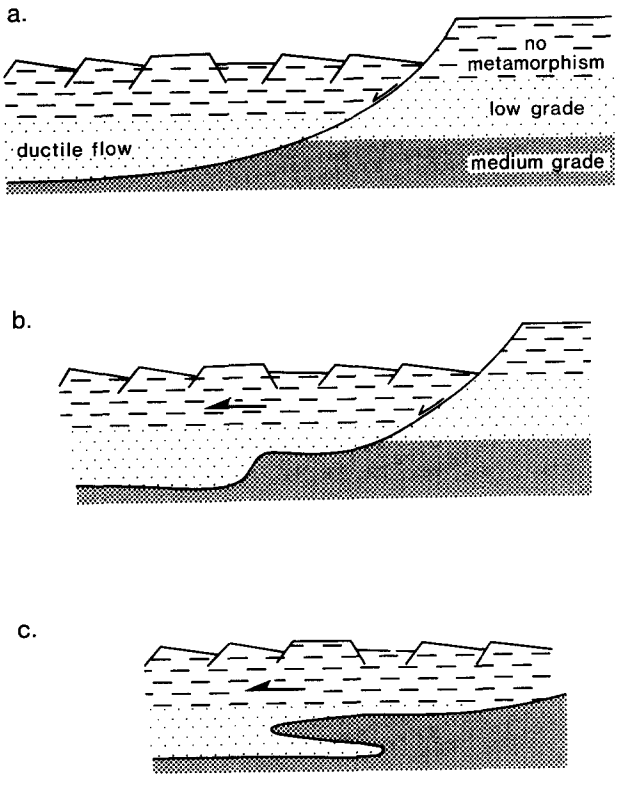

Fig. 17. Postulated evolution of PQ/black schist relations in the Aguilón nappe. (a) Listric normal faulting is induced by gravitational forces in a previously thickened tectonic pile undergoing prograde metamorphism. An extensional fault places low-grade phyllite from high in the pile onto medium-grade schist deeper down. (b) An internal buckling instability (Cobbold *et al.* 1971) develops in the fault during shear flow. (c) Fold amplifies into a tight recumbent structure as flow continues (Hudleston 1977). The fold then detaches along its lower limb and is emplaced as a fold-nappe.

The close association of the medium to low P/T ratio metamorphism described above with a high-temperature peridotite massif in the Serranía de Ronda led Torres-Roldán (1979) to invoke mantle diapirism to explain the Alborán thermal and topographic high. An alternative cause of topographic elevation is crustal shortening and thickening. Kyanite in Alpujarride rocks indicates burial to at least 15 km, and the glaucophanitic and eclogitic metamorphism of parts of the Nevado-Filabride requires tectonic burial to about 40 km. We

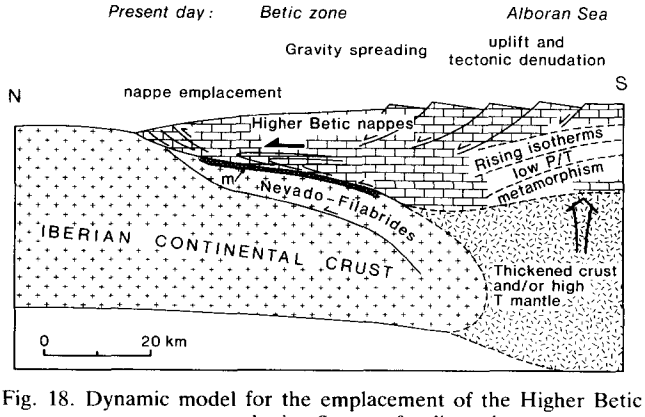

Fig. 18. Dynamic model for the emplacement of the Higher Betic nappes. m, mylonite. See text for discussion.

suggest that there were three phases in the tectonic evolution of the Betic Zone.

(1) Convergence between Africa and Iberia probably during the late Cretaceous to early Tertiary caused crustal shortening and thickening accompanied by high P/T ratio metamorphism in the Nevado-Filabrides and medium P/T ratio metamorphism in the future Alpujarrides. Thickened crust was isostatically uplifted.

(2) High-temperature peridotites were intruded, possibly in response to incipient rifting in the western Mediterranean area as a whole in Oligocene time (Hsü 1977). Further uplift was caused by the regional rise in temperature and this lead to the initiation of gravity spreading.

(3) There was gravity spreading of the Higher Betic nappes off the hot, thick welt of crust and high-temperature mantle, over the high-pressure Nevado-Filabrides and onto the Iberian continental margin (Fig. 18).

Acknowledgements—We are grateful to Claire Pope, Richard McAvoy, Suzannah Walters and Pat Jackson for technical and secretarial assistance. Discussions with José-Miguel Martínez, Miguel Orozco, Encarnita Puga, Reinoud Vissers and Jan Behrmann have greatly helped to clarify our ideas, and we thank the anonymous referees for their constructive comments on the manuscript.

REFERENCES

Andrieux, J., Fontboté, J. M. & Mattauer, M. 1971. Sur un modèle explicatif de l'arc de Gibraltar. *Bull. Soc. géol. Fr.* **7**, 115–118.

Akkerman, J. H., Maier, G. & Simon, O. J. 1980. On the geology of the Alpujarride Complex in the western Sierra de las Estancias. *Geologie Mijnb.* **59**, 363–374.

Bell, A. M. 1981. Vergence: an evaluation. *J. Struct. Geol.* **3**, 197–202.

Behrmann, J. H. & Platt, J. P. 1982. Sense of nappe emplacement from quartz *c*-axis fabrics; an example from the Betic Cordilleras (Spain). *Earth Planet. Sci. Lett.* **59**, 208–215.

Bourrouilh, R. & Gorsline, D. S. 1979. Pre-Triassic fit and Alpine tectonics of continental blocks in the western Mediterranean. *Bull. geol. Soc. Am.* **90**, 1074–1083.

Bucher, W. H. 1956. The role of gravity in orogenesis. *Bull. geol. Soc. Am.* **67**, 1295–1318.

Casey, M. 1980. Mechanics of shear zones in isotropic dilatant materials. *J. Struct. Geol.* **2**, 143–148.

Chapple, W. M. 1978. Mechanics of thin-skinned fold- and thrust-belts. *Bull. geol. Soc. Am.* **89**, 1189–1198.

Cobbold, P. R., Cosgrove, J. W. & Summers, J. M. 1971. The development of internal structures in deformed anisotropic rocks. *Tectonophysics* **12**, 23–53.

Cosgrove, J. W. 1976. The formation of crenulation cleavage. *J. geol. Soc. Lond.* **132**, 155–178.

Dewey, J. F., Pitman, W. C., Ryan, W. B. F. & Bonnin, J. 1973. Plate tectonics and the evolution of the Alpine system. *Bull. geol. Soc. Am.* **84**, 3137–3180.

Diaz de Federico, A., Gomez-Pugnaire, M. T., Puga, E. & Torres-Roldán, R. 1978. Igneous and metamorphic processes in the geotectonic evolution of the Betic Cordilleras (southern Spain). *Cuadernos Geol.* **8**, 37–60.

Dieterich, J. H. 1969. The origin of cleavage in folded rocks. *Am. J. Sci.* **267**, 155–165.

Egeler, C. G. & Simon, O. J. 1969. Sur la tectonique de la Zone Bétique (Cordillères Bétiques, Espagne). *Verh. K. ned. Akad. Wet.* **25**, 1–90.

Egeler, C. G., Rondeel, H. E. & Simon, O. J. 1971. Considerations on the grouping of the tectonic units of the Betic Zone, southern Spain. *Estud. Geol.* **27**, 467–473.

Elliott, D. 1976. The motion of thrust sheets. *J. geophys. Res.* **81**, 949–963.

Fletcher, R. C. 1977. Quantitative theory for metamorphic differentiation in development of crenulation cleavage. *Geology* **5**, 185–187.

García-Hernández, M., Lopez-Garrido, A. C., Rivas, P., Sanz de Galdeano, C. & Vera, J. A. 1980. Mesozoic palaeogeographic evolution of the external zones of the Betic Cordillera. *Geologie Mijnb.* **59**, 155–168.

Heim, A. 1919. *Geologie der Schweiz.* C. H. Tauchnitz, Leipzig.

Hermes, J. J. 1978. The stratigraphy of the Subbetic and southern Prebetic of the Velez Rubio–Caravaca area and its bearing on transcurrent faulting in the Betic Cordilleras of southern Spain. *Verh. K. ned. Akad. Wet.* **81**, 1–54.

Hoschek, G. 1969. The stability of staurolite and chloritoid and their significance in the metamorphism of pelitic rocks. *Contr. Miner. Petrol.* **22**, 208–232.

Hsü, K. J. 1977. Tectonic evolution of the Mediterranean basins. In: *The Ocean Basins and Margins, Volume 4A, The Eastern Mediterranean* (edited by Nairn, A. E. M., Kanes, W. H. and Stehli, F. G.). Plenum, New York.

Hudleston, P. J. 1977. Similar folds, recumbent folds and gravity tectonics in ice and rocks. *J. Geol.* **85**, 113–122.

IGME, 1973. *Geological Map of Spain, at* 1:50,000, *Tabernas.*

Kampschuur, W. & Rondeel, H. E. 1975. The origin of the Betic Orogen, southern Spain. *Tectonophysics* **27**, 39–56.

Kozur, H., Kampschuur, W., Mulder-Blanken, C. W. H. & Simon, O. J. 1974. Contribution to the Triassic ostocode faunas of the Betic Zone (southern Spain). *Scripta Geologica* **23**, 1–56.

Loomis, T. P. 1972. Contact metamorphism of pelitic rock by the Ronda ultramafic intrusion, southern Spain. *Bull. geol. Soc. Am.* **83**, 2449–2474.

Milnes, A. G. 1971. A model for analysing the strain history of folded competent layers in deeper parts of the orogenic belts. *Eclog. geol. Helv.* **64**, 335–342.

Nijhuis, H. J. 1964. Plurifacial Alpine metamorphism in the south-eastern Sierra de los Filabres south of Lubrin, SE Spain. Unpublished thesis, University of Amsterdam.

Platt, J. P. 1982. Emplacement of a fold-nappe, Betic Cordilleras, S. Spain. *Geology* **10**, 27–102.

Platt, J. P. & Vissers, R. L. M. 1980. Extensional structures in anisotropic rocks. *J. Struct. Geol.* **2**, 397–410.

Price, R. A. 1973. Large-scale gravitational flow of supracrustal rocks, southern Canadian Rockies. In: *Gravity and Tectonics* (edited by De Jong, K. A. & Scholten, R.). Wiley, New York, 491–502.

Price, R. A. 1981. The Cordilleran thrust and fold belt in the southern Canadian Rocky Mountains. In: *Thrust and Nappe Tectonics* (edited by McClay, K. R. & Price, N. J.). *Spec. Publs geol. Soc. Lond.* **9**, 427–448.

Ramsay, J. G. 1981. Tectonics of the Helvetic nappes. In: *Thrust and Nappe Tectonics* (edited by McClay, K. R. & Price, N. J.). *Spec. Publs geol. Soc. Lond.* **9**, 293–309.

Rao, B. & Johannes, W. 1979. Further data on the stability of staurolite + quartz and related assemblages. *Neues Jb. Min. Mh.* **1979**, 437–447.

de Roever, W. P. & Nijhuis, H. J. 1963. Plurifacial Alpine metamorphism in the eastern Betic Cordilleras (SE Spain). *Geol. Rdsch.* **53**, 324–336.

Rutter, E. H. 1976. The kinetics of rock deformation by pressure solution. *Phil. Trans. R. Soc.* **A283**, 203–219.

Torres-Roldán, R. 1974. El metamorfismo progresivo y la evolución de la serie de facies en las metapelitas alpujárrides al SE de la Sierra Almijara (sector central de las Cordilleras Beticas, Sur de Espana). *Cuadernos Geol.* **5**, 21–77.

Torres-Roldán, R. 1979. The tectonic subdivision of the Betic Zone (Betic Cordilleras, southern Spain): its significance and one possible geotectonic scenario for the westernmost Alpine belt. *Am. J. Sci.* **279**, 19–51.

Vissers, R. L. M. 1981. A structural study of the central Sierra de los Filabres (Betic Zone, SE Spain), with emphasis on deformational processes and their relation to the Alpine metamorphism. *GUA Papers of Geology*, Series 1, No. 15. University of Amsterdam, 1–154.

Weijermars, R. 1983. Definition of vergence. *J. Struct. Geol.* **4**, 505.

Westra, G. 1969. Petrogenesis of a composite metamorphic facies series in an intricate fault-zone in the south-eastern Sierra Cabrera, SE Spain. Unpublished thesis. University of Amsterdam.

Westerhof, A. B. 1977. On the contact relations of high temperature peridotites in the Serrania de Ronda, southern Spain. *Tectonophysics* **39**, 579–592.